EXPLORATIONS OF COMPLEX SOLID STRUCTURES USING THE GENETIC ALGORITHM

A Thesis

Presented to the Faculty of the Graduate School

of Cornell University

in Partial Fulfillment of the Requirements for the Degree of

Master of science

by

Xincheng Lei

August 2015

ABSTRACT

The genetic algorithm(GA) is an effective approach to predict material structures and explored theoretical energy landscape. In the thesis, the GA is applied to three complex solid structures, which are Aluminium-transition metal alloys, an amorphous phase and a thin film quasicrystal. Advanced or new prediction results are obtained by the package "genetic algorithm for structure and phase prediction(GASP)". Based on the results, properties and suitability of several atomic potential are discussed. Besides, finding new ground state of the Kob-Andersen binary mixture is a argument for the formation reason of preferred disordered phases in this model. Finally, some possible improvements of GASP are suggested to predict the complete structure of the thin film quasicrystal.

This thesis is dedicated to my adviser Prof. Christopher Henley and Prof. Neil Ashcroft. They not only guide me in the specific projects, but also teach me general principles in scientific research. I learned from them the long standing pursues after the truth and beauty of physics, no matter when and under what situation.

ACKNOWLEDGEMENTS

I would like to show deep gratitude to people helping me for the projects. Prof. Richard Hennig and his group provide me with the highly functional package (GASP) for genetic algorithm and powerful cluster server for simulation. Dr. Marek Mihalkovic gave me all the GPT and EOPP potentials and helped me with many computational technique details all through my research. Moreover, Prof. Michael Widom, Prof. David Muller, Dr. Eric Cockayne and Dr. Michael Engel gave me valuable suggestions and discussions.

TABLE OF CONTENTS

LIST OF TABLES

LIST OF FIGURES

Glossary of abbreviations

BLJ mixture - Binary Lennard-Jones mixture

DFT - Density functional theory

EAM - Embedded atom method

EOPP - Empirical oscillatory pair potential

GASP - Genetic Algorithm for structure and phase prediction

GPT - Generalized pseudopotential theory

KA binary mixture - Kob-Andersen binary mixture

MC method - Monte Carlo method

TM - Transition metal

CHAPTER 1

INTRODUCTION

From nano fabrication to aeroplane manufacture, advanced technology in various fields depends on innovation of new materials. The novel characteristics in electronics, optics, magnetism, thermodynamics and of their physical mechanism can be used to realize next generation of engineering. Numerical experiments have been carried out to search for new materials and characterize them. A successful experiment demands close control of many parameters including temperature, pressure, what is required for synthesis and details of the actual process. Experiment can be high consuming both for time and money, so it is significant to know more about the material before putting it into the laboratory.

Computational materials science is well suited for this kind of job. The strong computation ability of modern computer makes it possible to compute or simulate all properties, though with some limitation, before measurement in the laboratory. The simulation result can lead experiment into more prospective track. Sometimes experimental measurement is not feasible because the environment conditions do not allow it. Then computational methods can be a substitutive way. Besides, computation helps to understand the nature of material so that people can design novel materials accordingly.

Computational prediction for all properties is based on the electronic structure of the material. However, the prediction of structure itself is also a challenging but meaningful question. In recent tens of years, owing to first principle calculation and various algorithms for searching, there are numerous successful predictions leading to experiments afterwards. Nowadays three branches of structure prediction still attract computational physicists attention. The first one is materials under extreme conditions like high pressure. The second one is two dimensional materials or surfaces and interface property

of a bulk material. The last one is prediction of complex structures because bigger size brings in even larger complexity.

There are ”complex” structures in several modes. Crystal phases with large unit cell (above 20 atoms per unit cell for instance) are complex and difficult to predict. Quasicrystals[35] with long range order but no translational symmetry are complicated and difficult even to explain. Amorphous solid phases are more ”complex” by not having order at all.

In this thesis, some numerical methods along with qualitative explanation are tried for prediction and analysis of the three kinds of complex structures. In Chapter 5, a recently found thin film quasicrystal with associated difficulty of both complexity and dimensionality is discussed. Besides reporting successful prediction of a certain material, we also use the result to evaluate several theoretical models or potentials for these systems and try to get a deeper understanding of why there is or there is not long range order in aperiodic structure. In the last chapter, some proposals for improving the numerical method are put forward and discussed.

CHAPTER 2

ENERGY LANDSCAPE

Condensed matter might have atoms as many as Avogadro number of 10^{23}, which means it is in a thermodynamic limit. The equilibrium state of the matter should minimize the free energy of the system:

$$F =< E > -TS + PV \tag{2.1}$$

Here F is the Gibbs free energy. $< E >$ is the average internal energy of the ensemble. T is temperature, S the entropy, P the pressure and V the volume. Through out this thesis, we constrain our prediction to the condition $T \rightarrow 0$ (down to the ground state) and the pressure is around an atmosphere. By doing so, we do not need to consider thermal metastable phase in high temperature and phase transitions under high pressure. And, we do not discuss the degeneracy of ground state or entropy of low excited states, which are common in glass. Moreover, the dynamic contributions to the free energy including phonons in crystal and phason (counterpart of phonon in quasicrystal) are not discussed here. There are successful predictions by other groups including vibration and deformation of matter based on a knowledge of static atomic structure. However, our project focuses on the prediction of the static equilibrium structure.

So, the prediction turns into a mathematical question here namely how to minimize the ground state enthalpy:

$$H = E + PV \tag{2.2}$$

with variable atomic structure. There are six variable parameters of the unit cell as three lattice constant and three angles between lattice edges. For N atoms in unit cell, each one has 3 degrees of freedom (DOF) . Considering that a uniform shift of all atomic positions

will not change the structure, so the total DOF is 6 + 3N - 3 = 3N + 3. Every possible structure has a corresponding enthalpy. The hyper-surface of enthalpy in configuration space is called the energy landscape. So, our job is to find the high-dimensional optimization of the energy landscape.

Unfortunately, there is no exact analytic functional for the landscape. The Hamiltonian of condensed matter is:

$$\hat{H} = \hat{T}_{ion} + \hat{T}_{ele} + \hat{V}_{ion-ele} + \hat{V}_{ion-ion} + \hat{V}_{ele-ele} \tag{2.3}$$

Here $\hat{T}$ is kinetic operator while $\hat{V}$ is interaction operator. Since we only consider static stable phases, the kinetic Hamiltonian of ions can be initially ignored in the Born-Oppenheimer approximation ($\hat{T}_{ion} = 0$). But it remains a significant problem with many-body interactions of electrons (let alone the additional dimension associated with electronic degrees of freedom). Some numerical methods are demanded to approximate the Hamiltonian with effective atomic potential or at least a single-particle problem.

2.1 Density functional theory

Density functional theory (DFT)[1] is a powerful approach which transfers many-body electronic interaction into single-body particle density distribution. The density of electrons is defined as:

$$n(\vec{r}) = N \int d^3 r_2 \cdots \int d^3 r_N \, \psi*(\vec{r}, \vec{r_2}, \ldots, \vec{r_N}) \psi(\vec{r}, \vec{r_2}, \ldots, \vec{r_N}) \tag{2.4}$$

Here, $\psi(\vec{r}, \vec{r_2}, \ldots, \vec{r_N})$ is the wavefunction of N electrons. For a ground-state density $n_0(\vec{r})$, there is a unique ground-state wavefunction corresponding to it:

$$\psi_0 = \psi[n_0] \tag{2.5}$$

So, ground-state electron structure and corresponding energy can be calculated based on density of electrons. The ground state minimizes the energy, i.e, the density distribution minimizes the functional of energy.

$$E[n] = T[n] + U[n] + \int V(\vec{r})n(\vec{r})d^3r \tag{2.6}$$

Here, T term is kinetic energy, U term is electron-electron interaction and V term is ion-electron interaction. Then if the minimization of the functional E is achieved, the electronic structure and corresponding energy is obtained.

The interaction between electrons U can be traced into V to get a one-particle question. There is an approximation in this step relating to so-called exchange-correlation potential V_{xc}[1]. Several approximation in different levels are applied for the functional of V_{xc}. Then an iterative approach from initial guessing density function is used to solve the functional minimization. To be noticed, the density functional theory is a first principle method from electrons. Though with approximation of V_{xc}, it is the most accurate computational energy model we can use so far. Many empirical potentials are fitted by DFT.

2.2 Atomic potentials

The purpose of introducing atomic potentials is to see the relationships between potentials and phase structures more directly, both in computer simulation and analytic way. By removing the degrees of freedom of electrons, the computing speed of energy and corresponding optimization becomes tremendously faster. It makes some approaches for simulation and prediction possible at aspect of time scale. On the other hand, a simple and direct atomic potential might give a quantitative understanding of orders in short range and long range.

2.2.1 Embedded atom method

Embedded atom method[2][3]expresses the system energy in functions of interactions between ions and nonlinear interactions between ions and electron density from neighbouring ions. Physical basis of EAM is related to the second moment approximation to the tight binding theory. Given atomic positions r_i, the EAM potential is:

$$\begin{aligned} E_{tot} &= \frac{1}{2}\sum_{i,j}\phi_{ij}(r_{ij}) + \sum_{i}F_i(\bar{\rho}_i) \\ \bar{\rho}_i &= \sum_{j\neq i}\rho_j(r_{ij}) \end{aligned} \tag{2.7}$$

where ϕ_{ij} is the pair interaction between atoms i and j. F_i is the embedded energy on atom i. ρ_j is the contribution to the electron cloud from atom j at site of atom i. All these parameters can be fitted by DFT calculation on a database of phases. Usually there is no analytic function of ρ_j, F_i and ϕ_{ij}. They are expressed in splines with an appropriate cutoff. EAM is particularly successful model for metallic systems. In the thesis, two EAMs on Al-Co and Al-Cu binary alloys are applied for prediction of the phase diagram.

2.2.2 Pairwise potential

Pair potential is the simplest but a effective potential. Total energy is a function of only pair distance between all ions. The physical basis is Coulomb's force between two charges. In atomic solid, the Coulomb interaction can be regarded as between ions screened by electrons. In tight binding model, the screening effect leads to an exponentially decaying of the interaction on pair distance. Here the approximation is Thomas-Fermi approximation that external field from ions varies quite smoothly compared with electron's mobility. With nearly free electrons model, the back and forth

screening distribution leads to a long range Friedel oscillation[4] on pair distance. Then the approximation is from perturbation on planer wave expansion.

The accuracy of pairwise potential depends on if a more appropriate model with less approximation is applied. In the chapter 3, both the two pair potentials (exponential decaying one and oscillatory one) are applied for Aluminium-transition metal alloys. Result indicates the nearly free electron model is the more adaptive one through the energy landscape.

On the other hand, pair potentials are effective among molecules. The permanent and instantaneous electronic dipole-dipole interactions between two molecules are well described by van der waals forces. This model is successful to predict behaviours of molecular liquid phases and phase transitions to solid phases. In chapter 4, a particular Lennard-Jones style pair potential called Kob-Andersen potential is explored by GASP to search for its ground state.

2.2.3 Many-body interaction

Usually many-body effect appears in atomic potential. For screening effect, the electron cloud distributions are affected by all neighbouring ions meanwhile the Friedel oscillations even depend on the shape of Fermi surface. Hybridizations occur at the electron cloud overlapping also depends on many-body. So, a rigorous empirical potential should expand the total energy in pair terms, three-body terms, four-body terms and so on. Constrain in particular composition region makes it reasonable to neglect many-body effect to some extent[5]. It will be shown in the so-called empirical oscillatory potentials[6] in the chapter 2.

2.3 Numerical methods to explore energy landscape

Even with atomic potential, the energy landscape still remains high dimensional if complex structures are targeted. An efficient approach to explore the high dimensional space is demanded. Given a random structure, it can be relaxed into an optimized one by the gradient of the energy surface. However, gradients only leads to local minimums instead of the global minimum. A approach called local minimum hopping[7] has been applied to avoid attractions from local minimums. The hopping destinations can be chose randomly or in a certain pattern. For example, hopping to nearest local minimum is actually Monte Carlo algorithm.

The genetic algorithm [8][9] optimization is also a approach to explore the local minimums. The strategy of hopping has more physics basis. An new local minimum trial is decided by two good other good local minimums. By ”good”, it means lower energy. The physics information including short range orders and symmetries of the two local minimums is extracted and analysed to generate a new position in energy landscape. The rules of how to define ”good” local minimums and generate new one is the core question in the genetic algorithm which is introduced as follow.

CHAPTER 3

GENETIC ALGORITHM

3.1 Introduction

Compared with other brute-force methods, the genetic algorithm employs global update at each iteration by a large leap in energy landscape. Meanwhile, good local order with low energy can be keep during such leaps. A great deal of achievement on predicting crystal structure by genetic algorithm has been reported in the last decade years[10][11][12][13][14]. By regarding atomic structure as evolving, a simulation of evolution processes will select the fittest individual (in physical word, the structure with lowest energy) after some generations. This method appeared very successful for hydrogen containing compounds and inorganic compounds. For intermetallic compounds, complex phases with more than 12 atoms have rarely been predicted before.

There are already many practical attempts to realize an evolution numerically[15][16][17]. All important concepts in evolution theory including gene, reproduction, mutation and natural selection are expressed in various numerical methods. Here we are using a genetic algorithm package called GASP (genetic algorithm for structure and phase prediction), which was written and managed by Prof. Richard Hennig's research group.[17][18].

By recombination of genes from even different species, bacteria adapt quickly to new surroundings. Similarly, the genetic algorithm takes advantage of recombination of two structures toward lower energy ones. Besides, other evolutionary concepts including random mutation and gene duplication are also helpful and have been realized in GASP. The Fig.3.1 depicts one iteration consisting of several ways of generating new

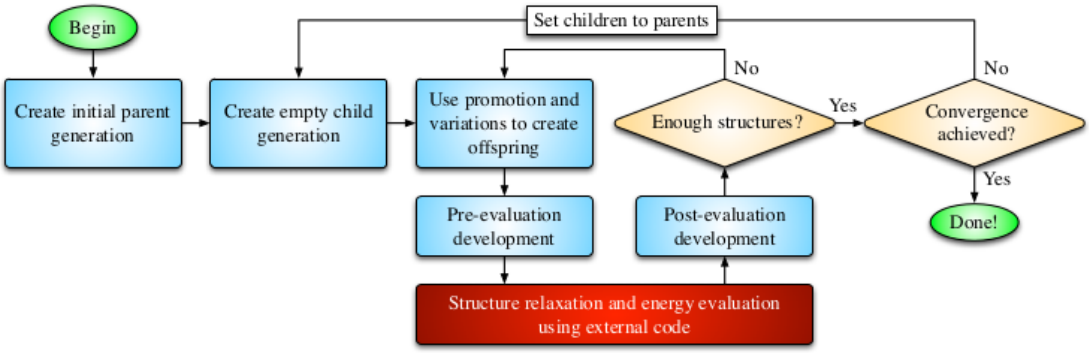

Figure 3.1: Process of genetic algorithm for optimization of atomic structures to lower energy. This figure is from [18]

trial structures and testing them.

3.2 Operations in GASP

”Promotion”, ”Slice”, ”Mutation” and ”Permutation” are four operations used on old structures to generate new structures. In detail, ”promotion” is to copy the several best old structures directly into the new generation. ”Slice” is realized by slicing (either planar or in a periodic wavy) two parent structures and merging the half of each one together to produce offspring structure. In large unit cells, this operation can keep the local order with suitable slice thickness and angle. So the slice operation guarantees the high heritability of local order. Like chromosome pairing, local order clusters are extracted from parents and recombined. In a single old structure, ”mutation” modifies both unit cell and atomic structure and ”permutation” is to exchange among different specie atoms. The opportunity of involving these reproduction is a control by a probability distribution based on the energy of structure. The closer it is from the convex hull, the larger chance it has to give plausible offspring.

Compared with Monte Carlo (MC) process, there are two main difference. Firstly, a group of structures, instead of only one in MC, are improving along GASP's iteration. Secondly, the giant leap in recombination ("Slice") operation can dramatically change the structure, which is not seen in MC. Mathematically, genetic algorithm is optimization on energy landscape. By "slice", the midpoint of two locally optimized configurations is assumed more possible to be the likely optimized configuration. The assumption is reasonable for energy landscape with a overall shape. It is a basic principle of the genetic algorithm that combination of two structures can keep good local order and lead to better long range order.

A example of "Slice" operation is shown in Fig. 3.2[18]. Consider a binary system consisting of two kinds of atoms, grey and blue. The formation energy is all pairwise interactions. Between the same kind of atoms, interactions are repulsive at nearest neighbouring distance and reach the minimum at the second nearest neighbouring distance. Between different atoms, interactions reach the minimum at the nearest neighbouring distance. Assume we already get two structures with low energy but not the ground state. In the figure 3.2 the two structures A (yellow and white) and B(green and white) are on the left. Inside every strip, the local order is good because different atoms are paired nearest. But, along the boundary, the same atoms meet close and lead to a high energy. The "Slice" operation keeps those good strip s and assembles them in a new combination. Now not only the inside pairs but also the boundary pairs are between different atoms. So, A globally optimized structure is obtained.

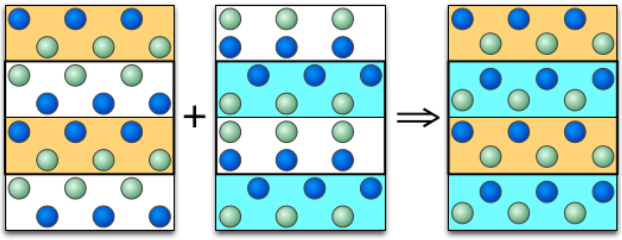

Figure 3.2: The operation ”Slice” lead to better globally optimized strucutre. The figure is from the author group of GASP[18]

CHAPTER 4

ALUMINIUM TRANSITION METAL ALLOY AND QUASICRYSTAL

As aluminium alloy, transition metal(TM) aluminides exhibits a wide range of physics properties which can be used for piratical application. With a low weight but high stiffness, it is broadly applied in aircraft. The compositions of Al alloy is well studied for engineering application, but there are still mysterious phases in the phase diagram such as Al13Co4 and Al3Cu4. Besides, aluminium transition metal is a main quasicrystal family. Since the first one AlMn was produced, many AlTM quasicrystals with icosahedral and decagonal phases have been found. So, study of atomic structures of AlTM crystal phases and quasicrystal approximant are helpful to understand this complicate metallic system.

In this chapter, three energy landscapes respectively based on three empirical atomic energy model are explored by genetic algorithm. Once the structure is identified, comparison with experimental known structure or calculating energy again with ab-initio method can evaluate the energy model in turn. Indeed, they show different suitability in different scale of region. After that, a comparison between short range order and long range order provokes a question against the previous idea of long range order in quasicrystal[19].

4.1 Energy model for prediction :Empirical potentials

Even with GASP, the prediction for a complex crystal structure is difficult because of the high dimensional configuration space for atomic structure. If prediction is based on little known information, there are many candidate structures all over the space to be tested. A simpler energy model, rather than DFT, can help to shorten the time for

one test and make the brute-force method possible. For the aluminium transition metal system, two empirical atomic energy models, embedded atom model(EAM)[2] and pair potential, are usually applied. In this thesis, one EAM potential and two kinds of pair potentials will be discussed.

4.1.1 Embedded atom method potential(EAM)

Based on tight binding theory, EAM potentials can describe metallic systems very well. The total energy is as follows in EAM form:

$$\begin{aligned} E_{tot} &= \frac{1}{2}\sum_{i,j}\phi_{ij}(r_{ij}) + \sum_{i}F_i(\bar{\rho}_i) \\ \bar{\rho}_i &= \sum_{j\neq i}\rho_j(r_{ij}) \end{aligned} \tag{4.1}$$

where ϕ_{ij} is the pair interaction between atoms i and j. F_i is the embedded energy on atom i. ρ_j is the contribution to the electron density from atom j at site of atom i. All these parameters can be fitted by Vienna Ab initio simulation package(VASP) in a molecular dynamics simulation. We use fitted EAM for Al-Cu and Al-Co from interatomic potentials repository project at NIST[20][21].

Both the electron density contribution function ρ_j and the embedding function F_i are fitted for each atom specie. So in different stoichiometry, the average electron density at each atom site varies because different species have different valence electron numbers. The strength of embedding energy also varies. The EAM potential is dependent of the composition.

Various properties in intermetallics can be predicted by this approach including lat-

tice constant, phonon dispersion relationship and plastic deformation. EAM can also do structure prediction by testing known structures to get the minimal energy one or running molecular dynamics or Monte Carlo for thermodynamic stability. However, EAM is rarely used for a prediction of crystal structure beyond simple structures. In this thesis, the genetic algorithm will be used to explore further possible structures to examine the suitability of EAM overall the energy landscape.

4.1.2 Generalized pseudopotential theory(GPT)

The GPT[5][22] is a first-principle generated potential serving for intermetallic systems of simple metals and transition metals, such as Al-Co. GPT expands total energy in terms of volume, pair potential and many-body potential. The volume term expresses the energy dependent of overall electronic density. The two and many-body terms express electron screening effect and sp, sp-d,d-d hybridizations. As a consequence, there are Friedel-like oscillatory tails among all interacting potentials, as shown in Fig.4.1. This is the main difference from the EAM potentials, which show no long-range oscillation. This oscillatory property is believed to lead to interesting structures in Al-TM system including some quasicrystals in the Al-TM family.

The hybridizations involving d orbital contribute many-body interactions. If nearest pairs of Co-Co with d-d hybridization exist, the many-body effect is very strong. Otherwise if there are only pairs of Al-Co with sp-d hybridization, the many-body effect becomes weaker. So, in the Al-rich region with few Co cluster, it is reasonable to neglect many-body potentials. The applications of only pair potential to Al-Co and Al-Ni can reproduce the phase diagram up to 25% composition of TM. So approximation should be therefore reasonable at this region. Above 25%, the calculated energy of Al5Co2

known stable phase hP28 is 0.06 eV/atom higher than experimental value. And another phase mP28 replaces hP28 as the stable one. The result also reflects the fact that only pairwise GPT is a efficient but not necessarily accurate potential model. A full GPT considering volume-dependence and many-body interaction proves to be necessary to modify it for more TM atoms. Actually, there are already 3-Co clusterss in Al5Co2. Approximation inclusive of many-body effect can be carried out by tracing over many-body effect into pairwise interaction. It is still an approximate model, but appears more accurate after fitting with VASP. Empirical oscillatory pair potential (EOPP) is such a fitting result which is introduced as follows.

4.1.3 Empirical oscillatory pair potential(EOPP)

EOPP is a fitted numerical potential by VASP for Aluminium transition metal compounds. It is an advanced version of GPT. The volume term is neglected because EOPP is defined on fixed density. The many-body effects are traced over into pairwise interaction. So, the fitted functional only contains pair potentials as follow:

$$V(r) = \frac{C_1}{r^{\eta_1}} + \frac{C_2}{r^{\eta_2}} \cos(k_* r + \phi_*) \tag{4.2}$$

The reasons of using decay with oscillations as EOPP function are from its physical meaning. Based on the same physical concept with GPT, EOPP[6] also contains Friedel oscillation from electron screening effect and hybridizations among s, p and d orbitals. The fitting process is via a high temperature molecular dynamics simulation which makes sure the sample is sufficiently diverse. The Co-Co interaction is obviously weaker than that in the GPT, as shown in Fig.4.1. The EOPP has already been shown to be successful for describing Al-TM system, even for quasicrystal. In the Results section, the genetic algorithm will show EOPP is actually valid for broader region in the phase

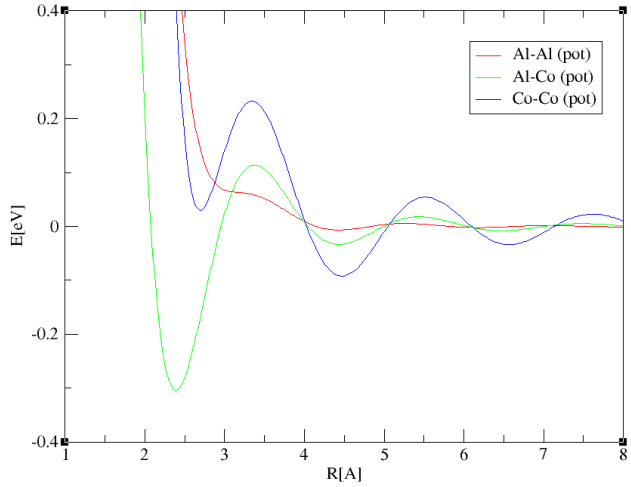

(a) GPT

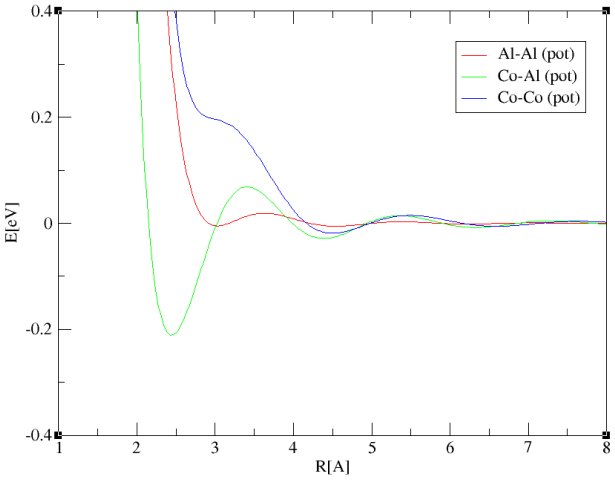

(b) EOPP

Figure 4.1: (a)GPT interatomic pair potential for Al-Co at Al-rich composition(b)EOPP for Al-Co at Al-rich composition

diagram.

4.2 Results

AlCu and AlCo binaries are our prediction targets. In AlCu, the expected stable phases are Al(cF4), Al2Cu(cF12), AlCu(mC20), Al4Cu9(cP52), Al1Cu3(tI8) and Cu(cF4). In AlCo, they are Al(cF4), Al9Co2(mP22), Al5Co2(hP28), AlCo(cP2) and a mysterious Al13Co4 phase. After the genetic algorithm efficiently explores the energy landscape of EAM, GPT and EOPP, except Al4Cu9(cP52) and Al13Co4, all expected stable phases are well predicted. However, along with them, competing structures with close to or even lower energy also appear, especially for the EAM potential. VASP calculations on them indicate the empirical energy is wrong and they are not really low energy structures. These misguiding competing structures leads GASP to a local minimum in energy landscape, which is partial reason for prediction failure. Relatively, GPT and EOPP appear more accurate over the whole energy landscape by which complex structures are successfully predicted.

4.2.1 Predictions for embedded atom method potentials

After running GASP on AlCu and AlCo based on EAM potentials, we obtain a convex hull for this energy model, which is roughly similar to the experimental one. In Fig. 4.2 they are displayed together. All known stable phases within 12 atoms can be predicted even though some of them are above the convex hull. Besides the expected stable phases, GASP found some more 'stable' phase than the known ones, but an energy calculation by VASP indicates they are not stable. As a second order approximation of tightly bound model, the EAM does not consider interactions between electrons and thus no electronic screening effect. However, to mid-range distance in Al-TM alloys, the screening effect is strong and significant for the crystal structures.

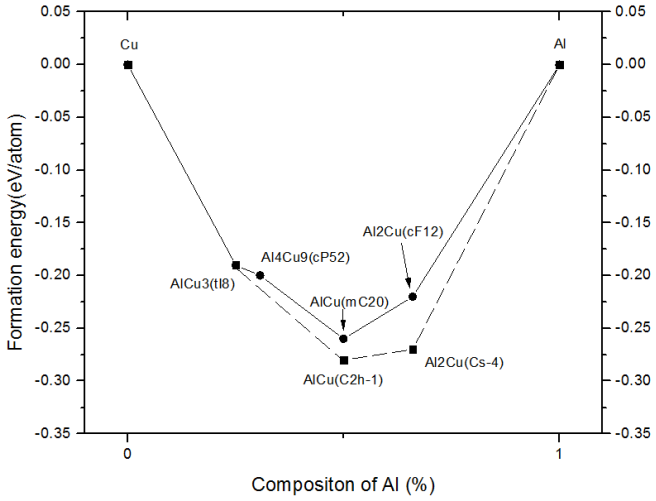

(a) Convex hull of AlCu

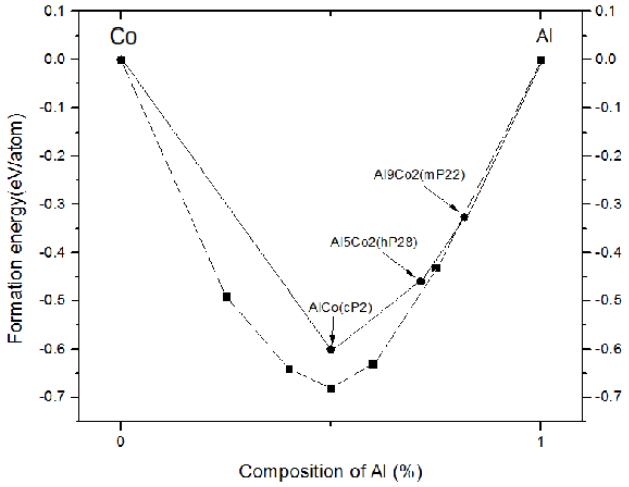

(b) Convex hull of AlCo

Figure 4.2: solid line and • is convex hull of experimental known stable phases; dashed line and ■ is convexl hull of 'stable' phases from GASP

In AlCu, the competing structures are AlCu(Pmm2) and Al2Cu(c2m)(see Fig. 4.3) These structure patterns dominate in the EAM potential calculation at different composition by tuning the center atom between Cu and Al. VASP calculations on both indicate that EAM underestimates the energy of competing structures with a difference of 0.09 and 0.18 eV/atom respectively. As will be seen, the densities of the competing structures and experimental known ones are very close. But the non-uniform local density in BCC

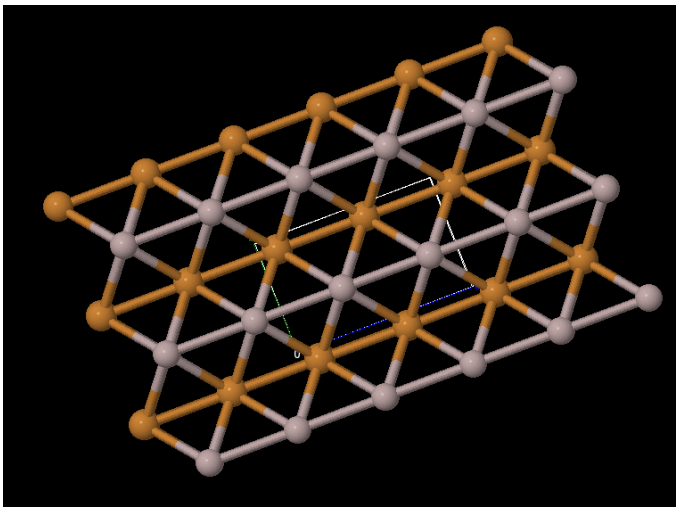

(a) AlCu

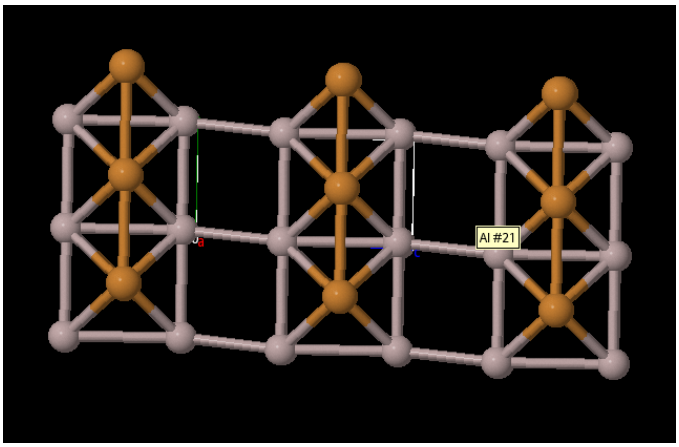

(b) Al2Cu

Figure 4.3: For EAM, competing structures with lower energy than known structures.Yellow atoms are copper and grey atoms are aluminium

and interval is quite different with uniform density in the known structure.

In AlCo, there are more competing structures. Al1Co3(P4/mmm) and Al2Co3(I4/mmm) are Co-rich and are not expected. On the other side, Al3Co1(P4/mmm) and Al3Co2(I4/mmm) also appear as stable phases. Including AlCo(I4/nmm), they are all similar structures having layers of body-centered cubic (BCC) separated by distorted cubics. Occupation at each site varies to give different composition. Again, the overall density is close to that of the known ones.

Table 4.1 compares the energy from EAM with the energy from VASP for those phases. We can see that EAM potential, though well fitted by ab-initio at known structure, may be incorrect at least somewhere on energy landscape. This was to be expected because EAM is designed for crystal structures near the known one. Elastic properties can be well described and a prediction of phase starting from known structure works well. However, a GASP calculation running without any previous information will likely flow into improper region in EAM energy landscape.

An newly invented adaptive genetic algorithm solves this problem by adapting EAM parameters every generation to the current explored region in the landscape[23]. It works but it also indicates no single EAM can describe all possible structures. However, we will see that oscillatory pair potentials can serve for a much broader region (maybe the whole landscape).

Formula	EAM energy	VASP energy	volume per atom
AlCu(cH2)	-0.27eV	-0.18eV	13.79 $Å^3$
AlCu(mC20)	-0.26eV	-0.21eV	14.03 $Å^3$
Al2Cu1(cS4)	-0.28eV	-0.1eV	14.83 $Å^3$
Al2Cu1(cF12)	-0.21eV	-0.15eV	14.84 $Å^3$
AlCo(cP2)	-0.63eV	-0.61eV	11.61 $Å^3$
AlCo(I4/nmm)	-0.69eV	?	11.94 $Å^3$

Table 4.1: phases with EAM low energy is prove to actually have higher VASP energy. Phases with close EAM energy also have close density.

4.2.2 Predictions based on empirical pair potentials

They are considered together because the physical base of them are the same. They both describe systems considering electron screening effects and hybridization among s,p,d orbitals. So they both have long range oscillatory tails. The only difference comes from the fact EOPP is fitted by VASP while GPT is given from analytic derivation. After

fitting, EOPP shows three main differences as follow: 1)GPT has a nearest neighbouring minimum for Co-Co pairs while EOPP does not; 2)The magnitude of the oscillations for Co-Co pairs is much larger than that for EOPP; 3)The wavelengths of oscillation are slightly shifted for Co-Co pairs.

Except from these differences, GPT and EOPP are more common with each other by possessing long range oscillatory tails. This property makes them very selective potentials. Not only short range orders but also middle range orders are constrained by the long range potential, especially the first positive peak. Three complex structures Al_9Co_2 mP22 phase, Al_5Co_2 hP28 phase and $Al_{10}Cu_{10}$ mC20 with above 20 atoms have been successfully predicted. Here the two AlCo binaries will also be discussed as examples.

We have run GASP on AlTM system in a given unit cell from experiment information. The volume-term in pair potential is usually given as a strong parabolic form minimal at known volume. An additional gradient algorithm for volume term is needed for relaxation. For simplicity, we carry out predictions based on a known unit cell. As mentioned before, many-body interactions can be neglected at Al-rich situation, so only pair interaction term remain.

4.2.3 AlCo phases

In AlCo, after around 5 and 20 generations, Al_9Co_2 and Al_5Co_2 appear respectively. The successful prediction owes itself to strong selective long range character of the potential. In Fig. 4.44.54.6, the pair distribution with each potential are shown. Al-Al and Al-Co pair distribution match both potential very well for Al5Co2. Especially, the pair distribution at the first positive peak of Al-Al and Al-Co pair is small. However, for Al9Co2, Co-Co pair distribution matches the the best while Al-Al distribution appears

at first peak.

Here the pair distribution is from counting all pairs in the structure to certain cut-off (usually 8 Å). Then a uniform distribution is obtained by normalizing numbers of pairs. This approach is used for pair distribution both in predicted structures and known structures.

From above, there appears to be a frustration between different pairs. It's impossible to satisfy pair potential for each three kinds of pairs. Al-Co interaction is the strongest one which demands certain Al-Co distribution in its minimum wells. For the rest two, even though GPT has stronger Co-Co interaction, the frustration between Al-Al and Co-Co still exists since Al-Al pairs are far more than Co-Co pairs. But, a counter-intuitive fact is that the Co-Co match dominates at Al9Co2 instead of Al5Co2. That is because a good match to a oscillatory potential is easily done when there are no clusters, in other words, the TM atoms are dilute. So, it supports usual concept that strong TM-TM pair potential leads to long range order of TM atoms if only it's very Al-rich composition. Then aluminium has just filled in the space between TM atoms.

Since there is a frustration between Al-Al and Co-Co pair potential around 70% aluminium, it's very important to get correct interacting strength to see which side dominates. Obviously, GPT and EOPP will give different result here since big difference in Co-Co interaction. The genetic algorithm incorporates this judgement by giving a competing structure (mP28) with nearly the same energy of Al_5Co_2 hP28 phase on GPT. On the other hand, there are no competing structures within 50 meV/atom using EOPP.

Fig. 4.7 shows the pair distribution of the competing structure which fit Co-Co interaction better than hP28 phase with a sacrifice on Al-Al interacting energy increase. Table 4.2 shows the energy in parts of Al-Al, Al-Co and Co-Co interaction. Using GPT,

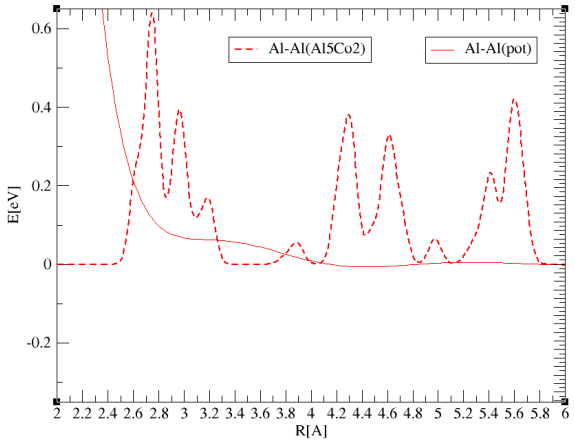

(a) Pair potential of Al-Al and corresponding distribution

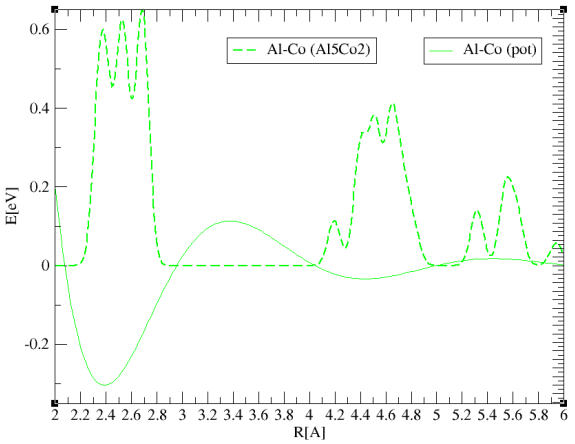

(b) Pair potential of Al-Co and corresponding distribution

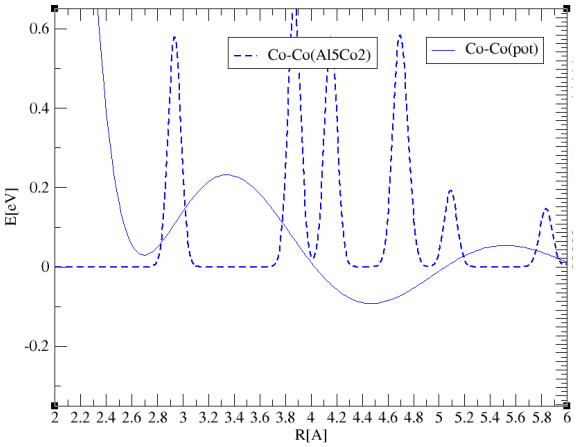

(c) Pair potential of Co-Co and corresponding distribution

Figure 4.4: Pair distribution of Al_5Co_2(known phase hP28) and potential of GPT. Al-Al and Al-Co distribution fit potential very well; Co-Co has distribution at first positive peak

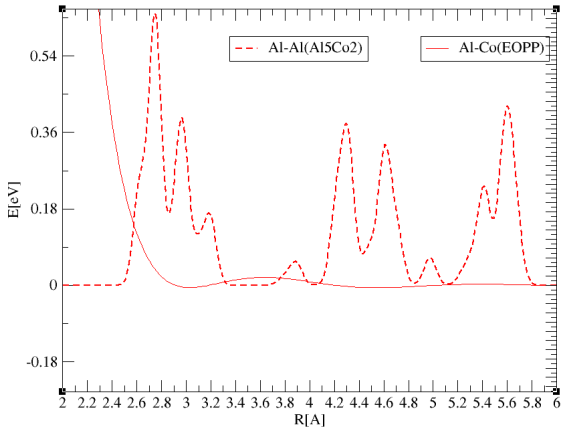

(a) Pair potential of Al-Al and corresponding distribution

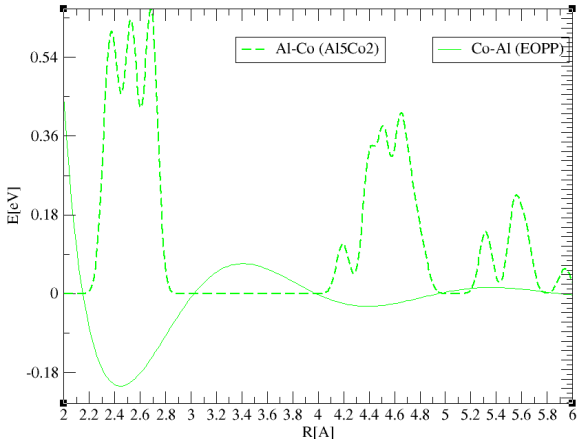

(b) Pair potential of Al-Co and corresponding distribution

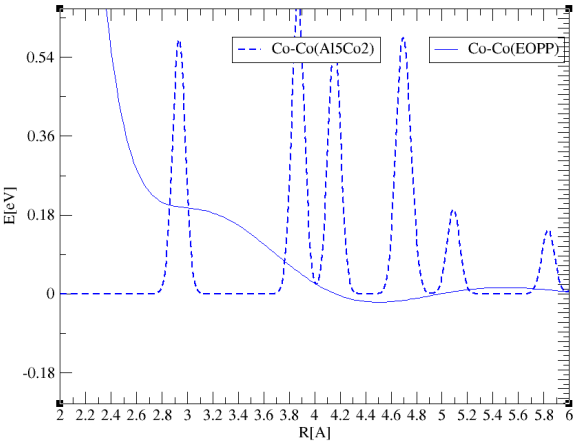

(c) Pair potential of Co-Co and corresponding distribution

Figure 4.5: Pair distribution of Al_5Co_2(hP28) and potential of EOPP. Al-Al and Al-Co distribution fit potential very well; Co-Co has distribution at first positive peak

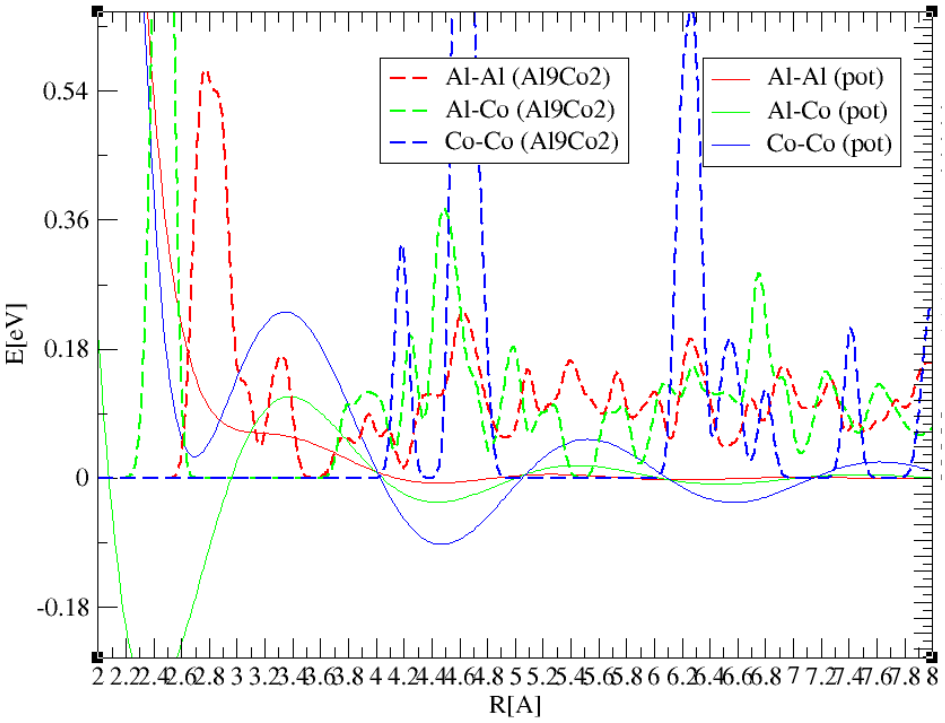

(a) Pair potential of GPT and corresponding distribution

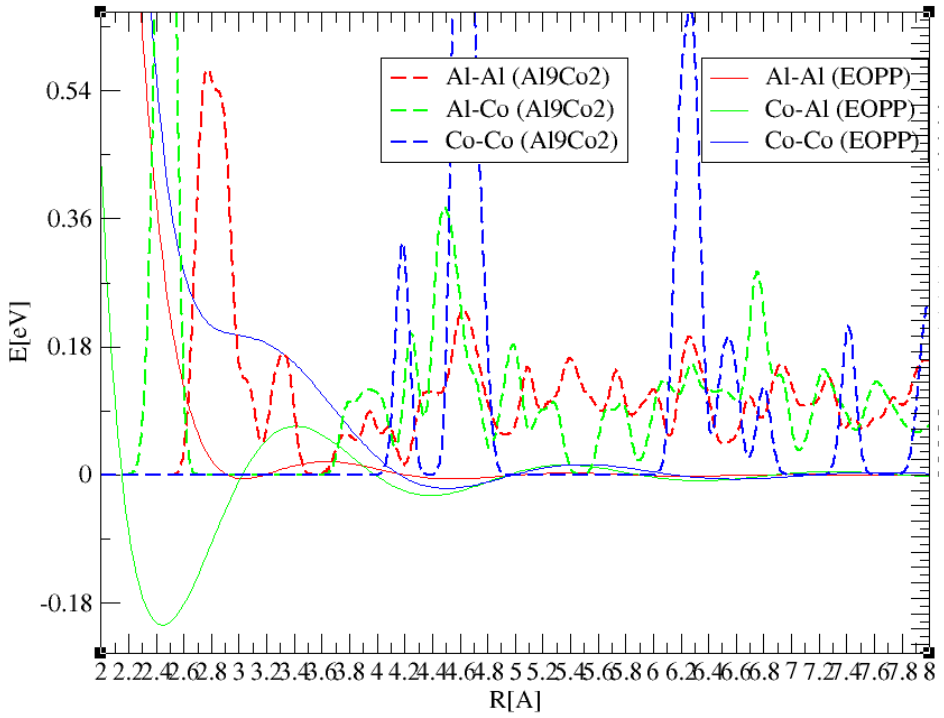

(b) Pair potential of EOPP and corresponding distribution

Figure 4.6: Pair distribution of Al_9Co_2 and potential of (a)GPT (b)EOPP. Al-Al and Co-Co distribution fit potential very well; Al-Co has distribution at first positive peak

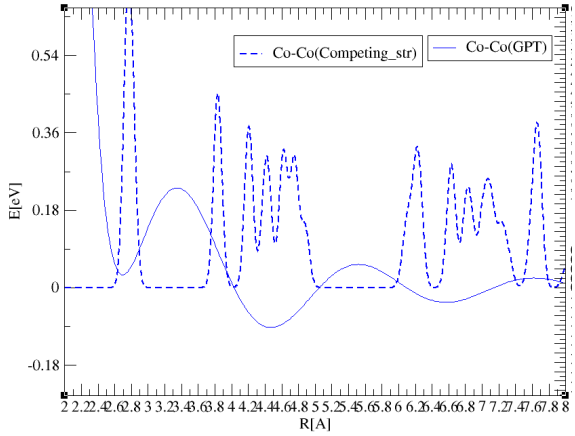

(a) Pair potential of Co-Co in GPT and corresponding distribution

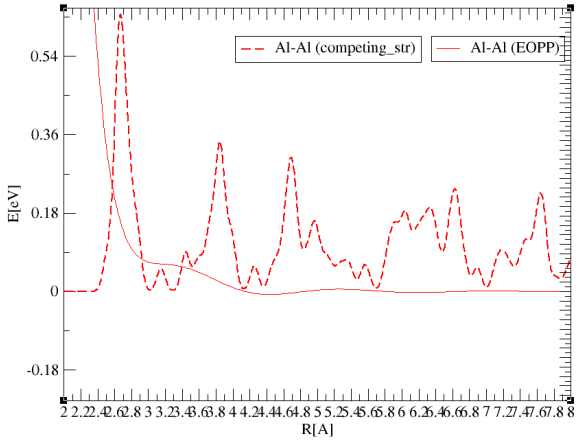

(b) Pair potential of Al-Al in GPTand corresponding distribution

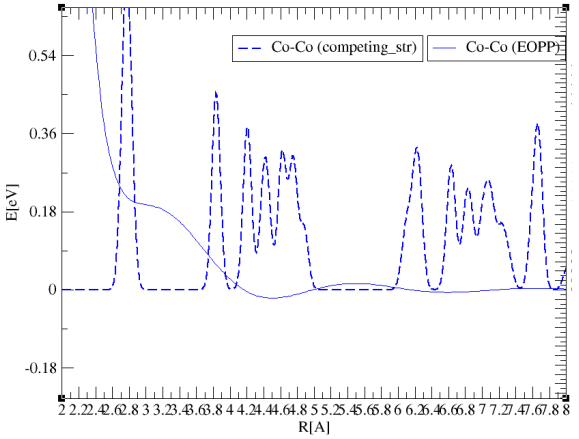

(c) Pair potential of Co-Co in EOPP and corresponding distribution

Figure 4.7: Pair distribution of Al_5Co_2(new phase mP28) and potential (a)potential is GPT, Al-Al and Co-Co distribution fit potential very well; Al-Co has distribution at first positive peak. (b)potential is EOPP, Co-Co does not fit so well with EOPP

the energy increased of Al-Al equals the energy decreased of Co-Co. Using EOPP, there is no change in Co-Co interaction and the total energy increases. Actually, both VASP and EOPP show that the energy of this competing structure should be 100 meV/atom higher than the known one. EOPP is more accurate and GPT overestimate strength of Co-Co interaction. So, it's the Al-Al interaction dominates at this region (30% TM).

GPT	total(eV)	Al-Al(eV)	Al-Co(eV)	Co-Co(eV)
hP28	-14.7496	9.6725	-23.5369	-0.8852
mP28	-14.2351	11.8818	-23.6194	-2.4974
EOPP	total(eV)	Al-Al(eV)	Al-Co(eV)	Co-Co(eV)
hP28	-14.0892	2.1394	-17.7513	1.5225
mP28	-11.2883	4.9711	-17.6714	1.6286

Table 4.2: Pair energy from each kind of pair in known structure and competing structure. The energy is on a unit cell basis, in which there is 28 atoms. GPT overstates the Co-Co strength and the negative interaction from Co-Co pairs

4.2.4 AlCu phases

Only $Al_{10}Cu_{10}$ mc20 phase is predicted. No competing structures are found. It indicates neglecting many-body effects for Al-Cu alloys can be valid to 50% composition of Cu, better than Al-Co alloys. However, the other complex phase Al_4Cu_9 (cP52) is not obtained after many GASP iterations. So far, the 52-atom unit cell phase is the bottle neck of GASP. In the last chapter, possible improvements in GASP are suggested to deal with it.

4.3 local structure vs. long range order

Considering the fact that there is a transition from Co-Co dominant to Al-Co dominant structures when composition of TM atoms is increasing, the long ranger Co-Co pattern is replaced by local order associated with Al-Co pattern. In Fig. 4.8(c), we can see the cluster surrounding one Co atom in Al_9Co_2 is not a particularly symmetric coordination shell. The distance to each aluminium is not restricted by Al-Co pair potential (especially the first peak). That is because Al_9Co_2 is at the Co-Co interaction dominant region in the phase diagram. Every TM atom is surrounded by all aluminium atoms without nearest TM neighbours. The strong Co-Co interaction leads to long range order among those TM atoms in each aluminium cage. Instead, the shape of the cage is not as important as the distribution of TM atoms. However, in Fig. 4.8(a),(b), two kinds of Co surrounded clusters both show very good symmetry and pair distribution of Al-Al fit the potential very well. So we can conclude that the local order (middle range up to 4Å) dominates at higher TM compositions and longer range order comes from matching rules of local order.

4.4 quasicrystals

Matching rule in AlCoNi decagonal quasicrystal[24] also support this viewpoint. Now Co(Ni) cluster is either star or boat or hexagonal tile. In each kind of tile, the structure is nearly already relaxed by EOPP. On the other hand, if we check the pair energy of TM-TM to a long range, we can find it's not the fittest distribution for only TM-TM pair potential.

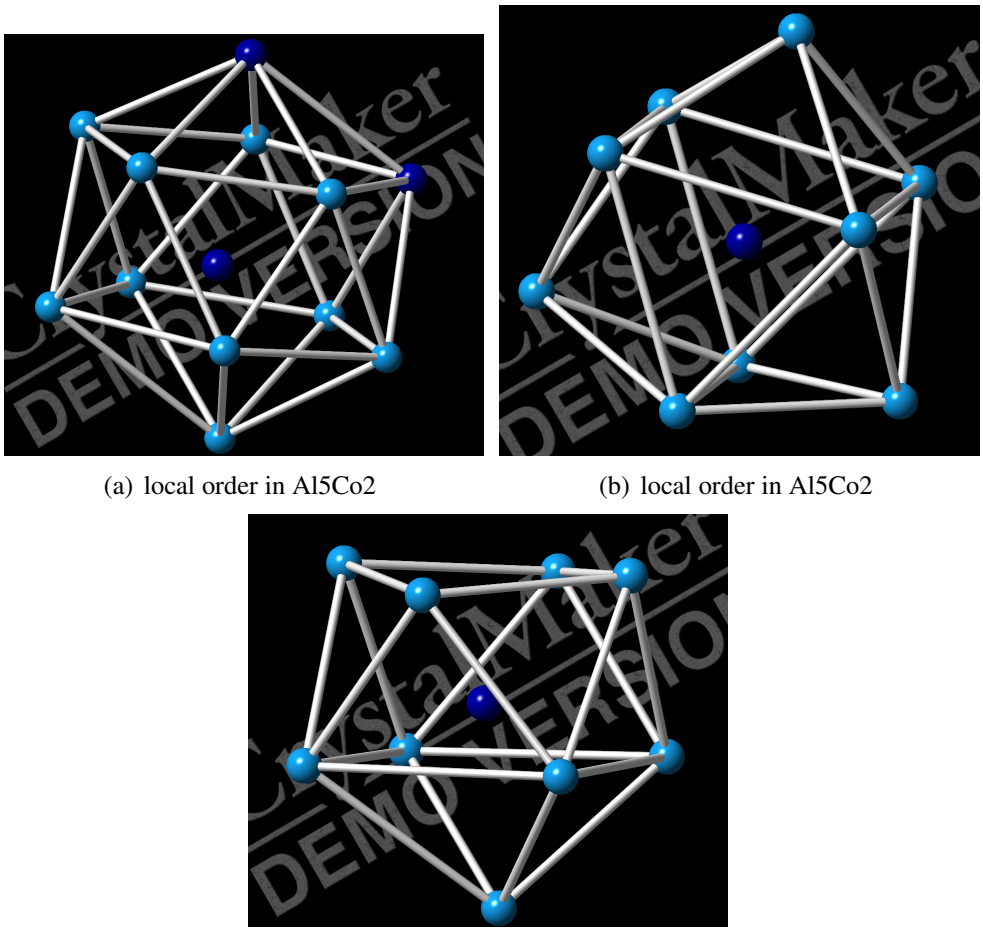

(a) local order in Al5Co2

(b) local order in Al5Co2

(c) local order in Al9Co2

Figure 4.8: Dark blue is cobalt atom and light blue is aluminium atom. (a)3-Co cluster in Al_5Co_2 (b)1-Co cluster in Al_5Co_2 (c)1-Co cluster in Al_9Co_2

CHAPTER 5

KOB-ANDERSEN(KA) BINARY MIXTURES

Amorphous solids are also non-crystalline structures. However, being different from a quasicrystal, amorphous state even lacks long-range order which makes it difficult to decide its atomic structure. Typical amorphousness phenomena are observed in glass, gels, thin films, etc. Glass is a special amorphous solid in which a phase transition from ordered state to disordered state has occurred. The formation of glass is related to many competing global states for frustration between local states. On the other hand, amorphous metals in thin films are produced by several methods in which the typical one is rapid cooling. Recently a critical slower cooling rate successfully produced an amorphous metal.

Kob-Andersen(KA)[25][26] binary mixture is a common amorphousness model for simulation. There are specifically designed Lennard-Jones potential interactions among the two kinds of atoms with specifically designed composition. The model is broadly used to simulate glassy transition. In timescale of molecular dynamics(MD), a liquid phase of this binary mixture will not be crystallized . Instead, a disordered solid phase is formed. The reasons could be either that there is not a crystalline ground state or that the diffusion barrier to the crystalline ground state is too big or that there are too many low energy degenerated disordered phases above ground state.

The first possible reason is denied because several crystalline ground state was found in the past one decade[27][28]. In this thesis, the genetic algorithm is applied to search for more low energy crystalline phases. One simple crystalline phase with only 10 atoms turns out to have much lower energy than known ones. Furthermore, discussion about the other two possible reasons is discussed later.

5.1 KA as a glass former

In system consisting of neutral atoms or molecules, Van der Waals potential has been successfully describing the interaction caused by instantaneously induced dipoles. In other hand, Pauli repulsion keeps atoms apart away in short range to avoid overlapping electron orbitals. The short rage repulsive interactions between molecules explain the pair correlation functions and the thermo-dynamics well. Previously the attractive parts of the potential only serve as perturbative cohesive background to keep molecules together. Recently research about the attractive parts indicates that they also have non-perturbative effect.

Lennard-Jones potential[29] is a popular mathematically simple model for these two kinds of interactions (van der Waals force and Pauli repulsion). Typically, the expression is in a form as:

$$V_{LJ} = 4\epsilon[(\frac{\sigma}{r})^{12} - (\frac{\sigma}{r})^{6}] \tag{5.1}$$

where ϵ is depth of the potential and σ is the distance at where the potential is zero. The distance at where the potential reaches the minimum is $r_m = 2^{1/6}\sigma$. The power law of 12 and 6 are both approximations for Pauili repulsion and van der Waals force. The electric filed induced by a instantaneous dipole is basically $\sim r^3$. In turn, the induced dipole will induce electric field back at the original instantaneous dipole which makes the power law to $\sim r^6$. However, the induced dipoles should be arouse by all dipoles around it. In Lennard-Jones potential, many body effect is ignored which makes it accurate. The power law of 12 is even more inaccurate. Simulation indicates that 12 can be replaced by another number ranging from $7 \sim 12$ in some cases. The more significant properties minimum distance and depth. By good fitting these two parameters, Lennard-Jones potential has been successfully explaining and predicting atomic structures in solid and liquid phases and the phase transition.

For mono-component system, the ground state of Lennard-Jones potential is hexagonal close pack structure. On rising temperature, it will turn into cubic close pack phase and then liquid phase. The binary mixture is more complicated for there are three sets of interaction with three depth and distance among two species. Kob-Andersen mixture is such a binary mixture of 80% big atoms A and 20% small atoms B with Lennard-Jones potential:

$$\begin{aligned} \epsilon_{AA} = 1.0; \epsilon_{AB} = 1.5; \epsilon_{BB} = 0.5 \\ \sigma_{AA} = 1.0; \sigma_{AB} = 0.8; \sigma_{BB} = 0.88 \end{aligned} \tag{5.2}$$

The specifically designed parameters are associated with a real amorphous phase $Ni_{80}P_{20}$ [30]. As a metallic glass, it does not show periodicity and long range order. Even the randomness pattern is still mysterious. Some local coordination information was proposed based on X-ray scattering[31]. Ab initio molecular dynamics also agree with the experimental data. The small atoms are usually surrounded by big atoms with a coordination number from 10 to 12. Different local B centered clusters are assembled together to form amorphous phase. The correctness of this suggestion is not guaranteed because all proposed structures are small scale due to simulation limit. However, Kob-Andersen potential, as an empirical potential for the binary, appears as a promising approach to simulate a much larger system.

Based on Kob-Andersen mixture model, correlation function in glass phase transition is well explained. In molecular dynamics, the model is reluctant to be crystallised which also agrees with the experiments. To explain it, the first step should be finding out the lowest energy crystalline phase.

5.2 Simple ground state of KA

Molecular dynamics already proves to fail to crystallize the Kob-Andersen mixture in regular time scale. Another approach, minimum hopping using techniques of basin-hopping and kinetic Monte Carlo steps[32][33] in energy landscape, was introduced to search for a ground crystalline state. Unlike the amorphous phase, possible crystalline phases show a pattern of clusters of closed packed structures containing B atoms and dilute area without B atoms. In Fig. 5.1, a low energy phases with 60-atom unit cell are shown.[34] There are two regions with different density divided by obvious boundary. The dense part consists of distorted B atom centered closed pack structures while the dilute part consists of distorted hexagonal structures.

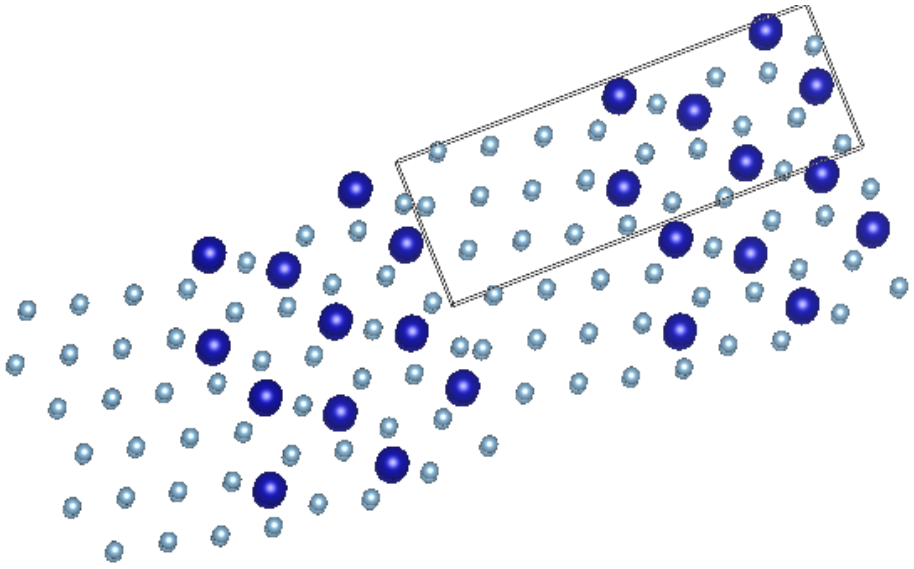

Figure 5.1: A crystalline phase from minimum hoppoing method with 60-atom unit cell

From GASP, a similar crystalline phase is predicted with much lower energy than the previous one. It is a simple 10-atom unit cell phase also with two density part. However, the spacing of dense part is two times of the dilute part and the boundaries between two

parts fit better. Every B atom is surrounded by 9 A atoms in a triangle cage. The local structure also matches better with the depth distance. Compared with the 60-atom unit cell, there are less distortion on the boundaries between dense and dilute regions.

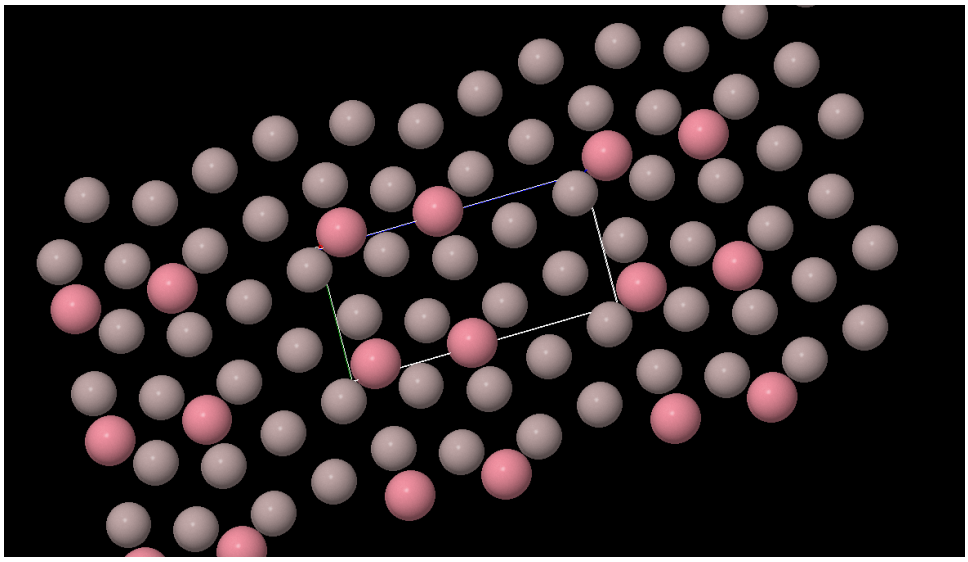

Figure 5.2: A crystalline phase from GASP with 10-atom unit cell

In Fig. 5.3, the energetic information of structures from GASP and other approaches are shown. There are hundreds of similar structures in the region from -8.4 eV/atom to -8.7 eV/atom. Most of them can be characterized as clusters of close pack structures of two species and regions in between with pure A atoms and lower density. Common local structures in the close pack regions are B atom centered cages of 7 8 A atoms. To be noticed, the coordination number is obviously smaller than our 10-atom unit cell one whose is 9. However, all structures, including crystalline phases from both GASP and minimum hopping and even amorphous phases, have the same density of 1.2 unit volume per atom! It remains mysterious that why structures with different energies prefer the same density even some of the them are inhomogeneous distributed. Also, further optimized structures with lower energy than -8.9 eV/atom might be found as larger unit cell. In our searching, the largest unit cell is 60-atom and no better phases appear.

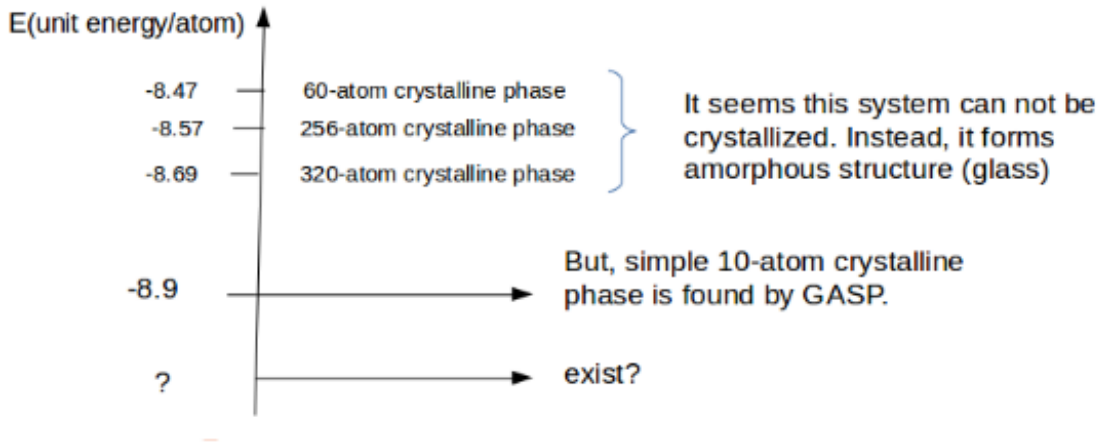

Figure 5.3: energies for several low energy crystalline phases

The discover of 10-atom unit cell low energy crystalline phase is a strong argument for the question why KA binary mixture prefers amorphousness. Since crystalline ground state exists, the reason should be entropic. In the real material $Ni_{80}P_{20}$, the liquid phase density is homogeneous. In solid ground state, there are two layers of dense parts separated by one layer of dilute part which has much lower entropy than amorphous phase. By diffusion, it has too small probability of getting into the ground state. In the perspective of simulation, GASP has two advantages over other approaches. The first is keeping good local structures (here are the triangle cages of A atoms). The second is slicing to find a good way to eliminate boundary defect between good local structures. By these two factors, GASP appears to be efficient to find highly ordered low energy phases.

CHAPTER 6

THIN FILM QUASICRYSTAL

In chapter 4, we discussed Aluminium-transition metal alloys and corresponding quasicrystal. Many quasicrystal exist in aluminium alloys such as Al-Ni-Co, Al-Cu-Fe, Al-Pd-Mn, etc. Other compounds also can form quasicrystal such as Ti-Zr-Ni, In-Ag-Yb. Besides inter-metallic compounds, in the last decade, quasicrystal on soft-matter has been broadly discovered to extend the species of quasicrystal. Recently, a totally new quasicrystal was reported. The perovskite BaTiO3 forms a 12-fold aperiodic thin film on a substrate of Platinum (111) surface[36]. Firstly, it is the first reported quasicrystal of oxide. Secondly, it is a two-dimensional quasicrystal on substrate. So, there should be new reasons for formation of this quasicrystal. Dimensionality, interface frustration between perovskite and substrate, forces from substrate and bonds involving oxygen are all possibly be effective for the formation.

6.1 experimental facts

BaTiO3 is sputtered onto the surface of Pt(111) at room temperature. It forms 3-dimensional islands separated by bare Pt terrace[38][39]. Then a high temperature annealing at 1250K in ultra high vacuum re-wet the bare Pt areas between the islands. The re-wetting covers the Pt with BaTiO3-derived quasicrystal. The low-energy electron diffraction (LEED) and scanning tunnelling microscopy (STM) both indicate the 12-fold symmetry. In the figure 6.1, a sharp 12-fold diffraction of electrons with 66eV energy is shown. In the figure 6.2, the top surface of the quasicrystal shows a 12-fold pattern consisting of the so called StampfliGahler tiling[37]. Square and triangle tiling are assembled to form a ideal dodecagonal pattern. The size of tiling is 6.85Å for edges

of squares and triangles. At the next level, dodecagons form a self-similar tilings with also squares and triangles.

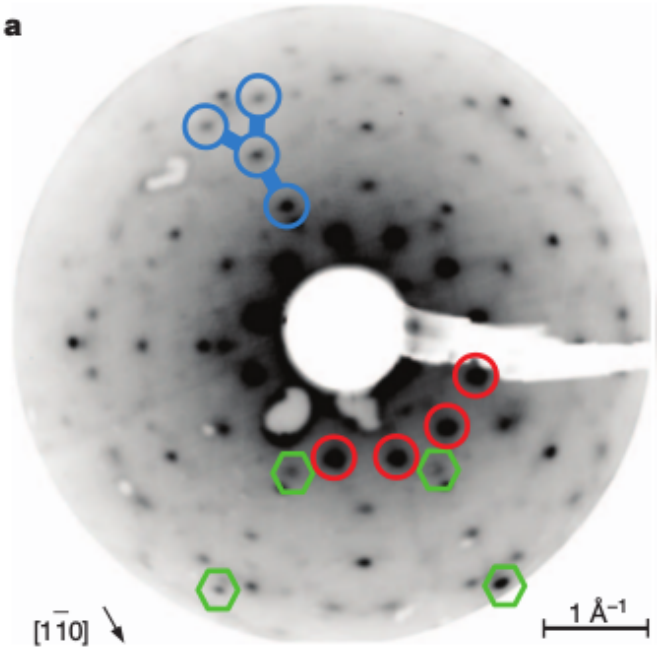

Figure 6.1: Sharp 12-fold symmetry in LEED pattern. The red and blue circles are first and second order diffractions from the dodecagonal quasicrystal and the gree circles are for diffractions from the bulk phase islands. This figure is from [36]

However, STM image does not indicate the species of atoms on the top and the structures beneath the top layer are not known. Actually, the accurate composition is also missing. An X-ray photonelectron spectroscopy (XPS) indicates that there are many Ti^{3+}s in the thin film quasicrystal while only Ti^{4+}s exist in the bulk phase islands. There are two possible reasons for valence changing. Firstly, at the interface the oxygen atoms can escape into vacuum or substrate. The oxygen vacancy corresponds to smaller valence of titanium. Secondly, if the Fermi-level of the substrate is higher than the bulk phase BaTiO3, electrons will flow into BaTiO3 and Ti^{4+}s are changed into Ti^{3+}s. The XPS result is the key to understand the formation of quasicrystal.

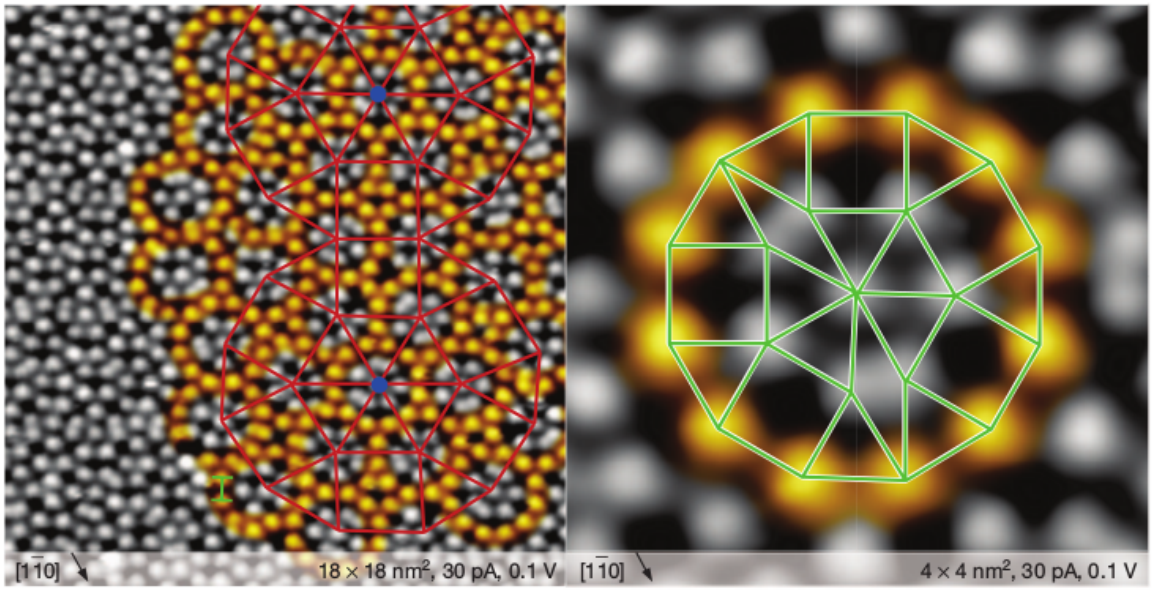

Figure 6.2: STM image of the quasicrystal top surface. Square and triangle tiling are motifs in the quasicrystal. Yellow marked atoms are shells of the first order dodecagons and the green lines draw the complete structure inside a dodecagon. The red lines draw the structure on the next level dodecagons. This figure is from [36]

6.2 Possible reasons for forming quasicrystals

The formation mechanism of this new quasicrystal still remains unknown. There are several factors which might be associated with the dodecagonal pattern. The substrate Pt (111) is a 3-fold surface while the quasicrystal is 12-fold. The incommensurate mismatch of symmetry and lattice constant is a possible situation where long range orders form. In the surface band structure of substrate, if the Fermi surface has regions close to planar, then the potential from surface Pt atoms can have long Friedel oscillatory tails just like in Al-TM alloys. Similarly, the long tails might lead to long range orders like dodecagonal pattern. Besides, the electrons might flow into thin film then dipoles form at the interface which would generate an interaction between quasicrystal and substrate. At last, oxygen vacancy which is already prove by XPS is a common reason for recon-

structions on thin film perovskite. Before producing the quasicrystal thin film, the same group grew a crystalline thin film with square and triangle tiling using similar experimental set up[40]. It is one of the oxygen-deficient ordered phase of BaTiO3 on Pt(111). However,previously reported reconstructions of SrTiO3 on Pt(111) surface from oxygen vacancy did not bring such a complexity in quasicrystal[41]. So, the formation reasons are multiple questions.

Before describing the effect from substrate, we focus on the last reason proposal, i.e., what is the two-dimensional phase of perovskite BaTiO3 (Of course the composition is roughly expressed because of atoms escape at the interface). The genetic algorithm is still promising in this prediction problem. However, several atomic potential[42][43][44] for bulk phase perovskite are tested, but none of them appears accurate on the whole energy landscape. Instead, the prediction should be conducted on the energy surface of density functional theory calculation. It demands very good optimization algorithm because one VASP calculation on even one dodecagon can be very time-consuming. So far, the GASP requires some improvements, which will be mentioned in next chapter, for the prediction task.

Instead of using GASP to realize the genetic algorithm in totally automatic way, a manual approach by inspection gives a proposal of the quasicrystal structure. The spirit is the same. Extract good local motifs and re-assemble them to get new ones. Bulk phases of BaTiO3 are: hexagonal, cubic, tetragonal, orthorhombic and rhombohedral structures. In the cubic phase, every Ti atom is surrounded by six O atoms in a octahedral way and Ti atoms form the cube. The Ba atoms are at the center of each cube. In low temperature stable tetragonal and orthorhombic, the crystal structure is very similar to cubic one but with distorted positions of Ba atoms and O atoms at the edges. In hexagonal phase, the octahedral structure of TiO6 still remains but O atoms can play

as the middle lay of a bi-pyramid of Ti2O3 instead of connecting Ti atoms as the edge middle.

From those bulk phase, some local structures can be extracted for possible motifs in the quasicrystal. For example, Fig. 6.3 and Fig. 6.4 show triangle and square motifs from bulk hexagonal phase. The edge lengths of those motifs are around 6.7 to 7.0 Å which is close to the length of tiling in the quasicrystal (6.85Å). The atoms near the motifs, especially atoms near the edges are called decorations[45]. They classify edges into different classes. Two motifs can be put together to share one edge only if the decoration on the edge is the same. In figure 6.5 and 6.6, five motifs with special decorations are shown. To be noticed, there are more kinds of motifs from bulk phase, not only in hexagonal phase. Of course, when being assembled together to get a two-dimensional structure, there are frustrations on edge decoration which distort the local structure of each motif. How to assemble motifs and how to modify them for better inter-motif mismatch can be solved by GASP. Since the prediction level rises up to motif, the possible combination will be much less to get efficient optimization speed. It is feasible by a improved GASP which can recognize the motifs and value the mismatch between them.

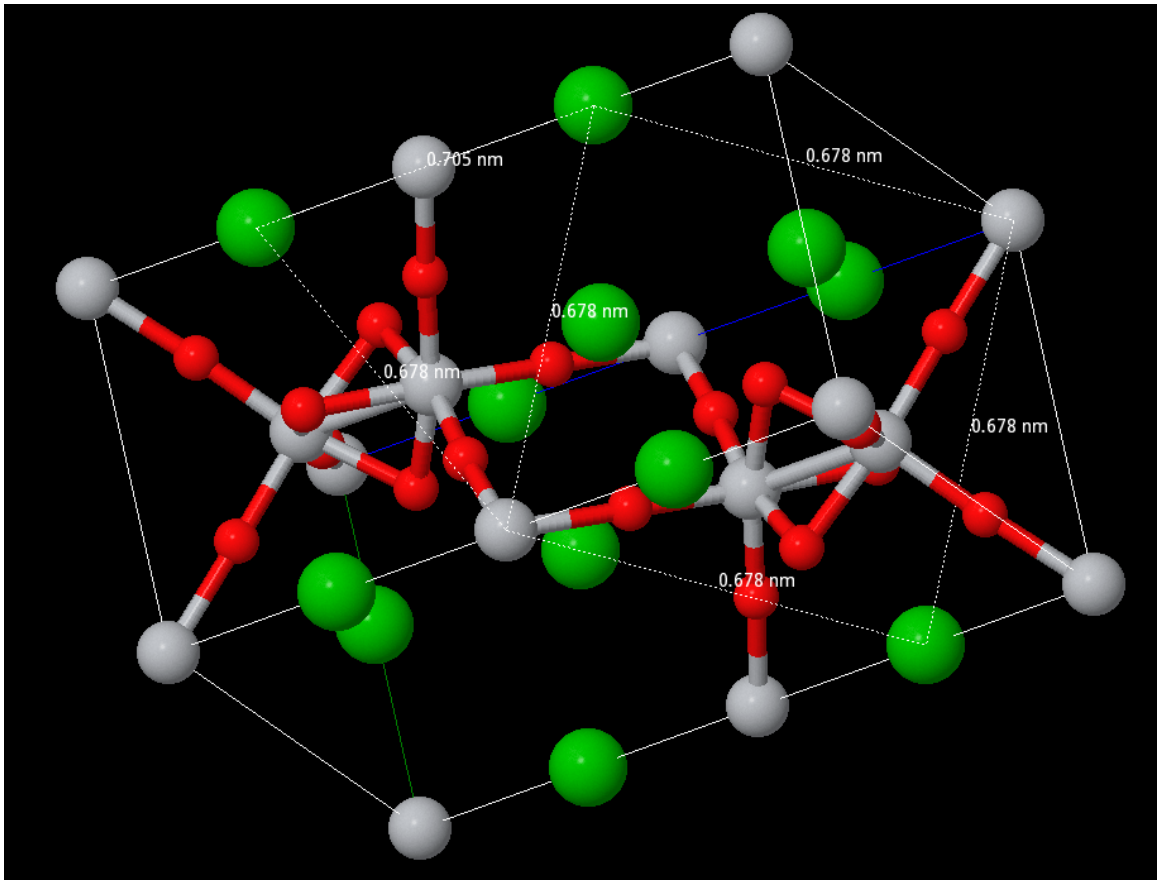

Figure 6.3: A square and triangle motif from hexagonal bulk phase. The green atoms are Ba, grey atoms are Ti and red ones are O. The length is shown on each edge

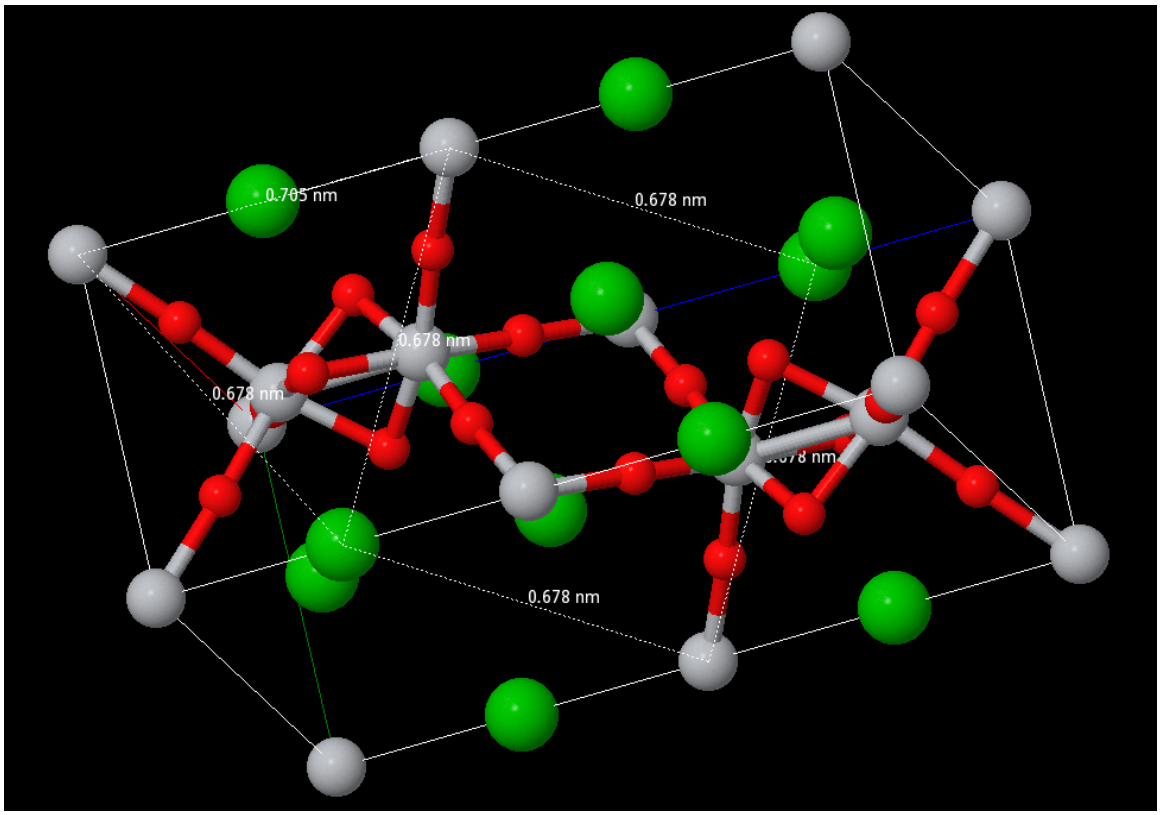

Figure 6.4: A square and triangle motif from hexagonal bulk phase. The green atoms are Ba, grey atoms are Ti and red ones are O. The length is shown on each edge

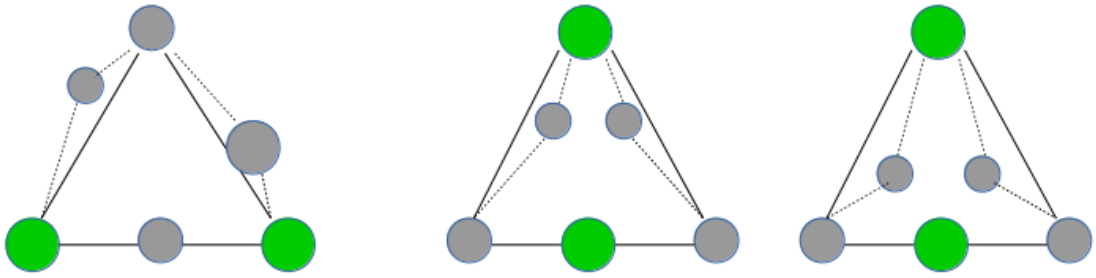

Figure 6.5: Three triangle motifs. The green circles are Ba while grey ones are Ti. The bigger atoms are above the motif surface while the smaller ones are beneath. There are two kinds of decoration: close to the Ba atom and close to the Ti atom. Two motifs can share the same decorated edge.

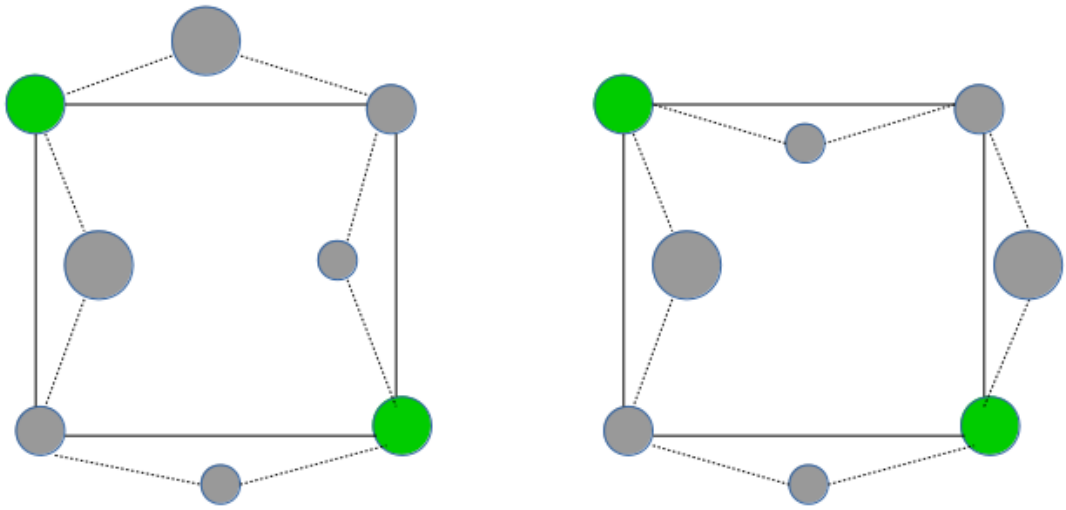

Figure 6.6: Two square motifs. The green circles are Ba while grey ones are Ti. The bigger atoms are above the motif surface while the smaller ones are beneath. There are two kinds of decoration: inside and outside. Two motifs can share the same decorated edge.

CHAPTER 7

IMPROVEMENTS OF THE GENETIC ALGORITHM AND SUGGESTION FOR FUTURE WORK

In conclusion, the genetic algorithm is a effective approach to predict complex atomic structures especially when there is little information for reference. Several Al-TM complex stable phases are predicted. In Fig. 7.1, previous works of the genetic algorithm on intermetallic compounds are shown[18]. The largest unit cell is below 10 atom per unit cell. The most complex structures in our result is $Al_{20}Co_8$ with 28 atoms per unit cell. So it is a big advance due to good wavy slice operations which keep good local structures. For Kob-Andersen binary mixture, it is also a big leap from pre-claimed ground state of -8.6 eV/atom to a lower one with -8.9 eV/atom. Although they both consist of separated phases. The new one has better atomic arrangement both inside the separated phases and on the boundaries. Still, the slice operation helps to give the highly optimized arrangement.

Compound	Pressure [GPa]	Formula units per cell	Energy code
Al-Sc system	0	8 atoms	VASP
	0	6, 8 atoms	VASP
	0	8 atoms	VASP
$Al_{13}K$	0	1	VASP
Au_2Pd	0	4	VASP
	0	4	VASP
$CaLi_2$	10-250	1, 2, 3, 4, 6, 8	VASP
$CdPt_3$	0	2	VASP
CuPd	0	4	VASP
Na-Ca system	50	Not specified	VASP
$PdTi_3$	0	2	VASP

Figure 7.1: Previous applications of genetic algorithm to intermetallic compounds. This figure is from [18]

However, limitations also appear in these applications. In Al-TM alloys examples, the prediction of structures with above 20 atoms per unit cell requires a known unit cell. Moreover, complex structures with above 50 atoms per unit cell have not been predicted even with known unit cell information. In the prediction of thin film quasicrystal, the algorithm should be improved tremendously the the usage of DFT energy calculation instead of atomic potential can be feasible. So far, some ideas for promoting GASP are proposed but need practical realization in the package.

7.1 More efficient crossover operation

Elser, Veit, and Christopher L. Henley. ”Crystal and quasicrystal structures in Al-Mn-Si alloys.” Physical review letters 55.26 (1985): 2883. Wavy oscillation is the most significant different operation in GASP compared with other genetic algorithm package. And it appears to be the key to advanced prediction result from GASP. In the future, the slice operation can be improved furthermore.

Firstly, the slice should recognize the boundary shapes of local clusters, then it can cut through the structure in a certain way to keep every cluster complete. Every boundary atoms should be shared by two or more clusters.

Secondly, the slice should not be constrained in single unit cell. If a good energy local structure is extended outside the unit cell, all atoms of it should be kept. When combining two structures, instead of using the average of the two unit cell, we should assemble the sliced local structures with the least distortion of them. The boundary atoms can be merged if needed and different combining directions can be tried for the best boundary match. In Fig. 7.2, it shows a improved combination operation.

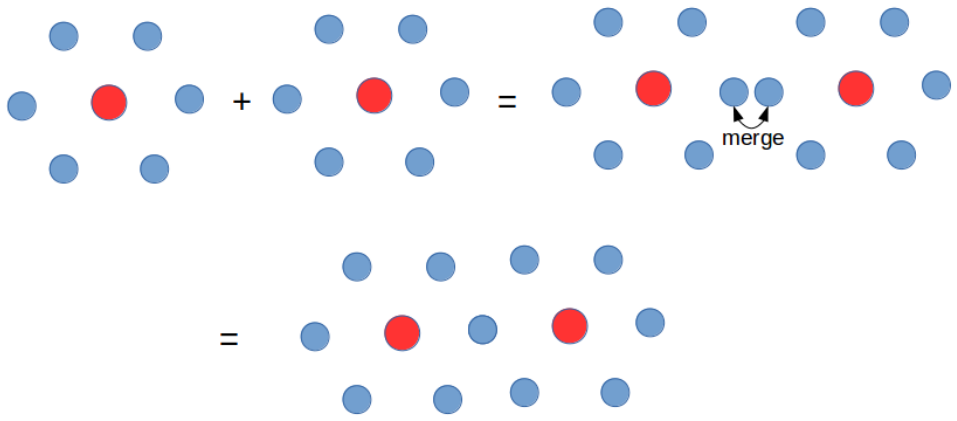

Figure 7.2: Finding a good combining edges and merging of very close atoms into one can help to get a further optimized structure

7.2 Evolution on levels of motifs instead of atoms

In new material prediction, sometimes the potentials strongly prefer a short range orders while sometimes we already know information of some motifs in the structure. In our projects, the Al-TM alloys have strong interactions between nearest neighbours which leads to certain order in TM atoms' clusters. The STM image of quasicrystal thin film already show the square and triangle motifs at the top surface.

If these clusters and motifs can be regarded as elemental units in replacement of atoms, then the searching for ground state is remarkably speeded up. For example, in the thin film quasicrystal, the motifs are squares and triangles with all possible atomic arrangement on vertices and edges. Instead of slicing a unit cell into layers (we do not even get a unit cell here), the motifs are proposed at the beginning and assembled together in a random way. The energy calculation for per atom is changed into energy for per motif. Cut out the better motifs with lower energy, assemble them in another random way.

This proposal might be appropriate for the thin film quasicrystal problem. Firstly, there are no unit cells to slice and any periodic operation would still lead to a crystalline one which is contrast to the real quasicrystal pattern. But usage of motifs will get larger and larger pattern without periodicity. Secondly, thin film matter is two dimensional which makes the proposal of assemble motifs together reasonable. It is a difficult task to build a structure by 3 dimensional bricks with uncertain shapes and boundary conditions. But in two dimension, it can be realized by basic machine learnings[46] [47].

BIBLIOGRAPHY

[1] Kohn, Walter, and Lu Jeu Sham. "Self-consistent equations including exchange and correlation effects." Physical Review 140.4A (1965): A1133.

[2] Daw, Murray S.; Mike Baskes (1984). "Embedded-atom method: Derivation and application to impurities, surfaces, and other defects in metals". Physical Review B (American Physical Society) 29 (12): 64436453.

[3] Daw, Murray S., Stephen M. Foiles, and Michael I. Baskes. "The embedded-atom method: a review of theory and applications." Materials Science Reports 9.7 (1993): 251-310.

[4] Friedel, J. "Electronic structure of primary solid solutions in metals." Advances in Physics 3.12 (1954): 446-507.

[5] J.A. Moriarty and M. Widom, "First Principles Interatomic Potentials for Transition Metal Aluminides. Theory and Trends Across the 3d Series", Phys. Rev. B 56 (1997) 7905-7917.

[6] Mihalkovi, Marek, and C. L. Henley. "Empirical oscillating potentials for alloys from ab initio fits and the prediction of quasicrystal-related structures in the Al-Cu-Sc system." Physical Review B 85.9 (2012): 092102.

[7] Goedecker, Stefan. "Minima hopping: An efficient search method for the global minimum of the potential energy surface of complex molecular systems." The Journal of chemical physics 120.21 (2004): 9911-9917.

[8] Goldberg, David E. Genetic algorithms. Pearson Education India, 2006.

[9] Fogel, David B. "An introduction to simulated evolutionary optimization." Neural Networks, IEEE Transactions on 5.1 (1994): 3-14.

[10] Woodley, ScottM, et al. "The prediction of inorganic crystal structures using a genetic algorithm and energy minimisation." Physical Chemistry Chemical Physics 1.10 (1999): 2535-2542.

[11] Oganov, Artem R., and Colin W. Glass. "Crystal structure prediction using ab initio evolutionary techniques: Principles and applications." The Journal of chemical physics 124.24 (2006): 244704.

[12] Tipton, William W., et al. ”Structures, phase stabilities, and electrical potentials of Li-Si battery anode materials.” Physical Review B 87.18 (2013): 184114.

[13] Zhao, X., et al. ”Exploring the Structural Complexity of Intermetallic Compounds by an Adaptive Genetic Algorithm.” Physical review letters 112.4 (2014): 045502.

[14] Woodley, Scott M., and Richard Catlow. ”Crystal structure prediction from first principles.” Nature materials 7.12 (2008): 937-946.

[15] Glass, Colin W., Artem R. Oganov, and Nikolaus Hansen. ”USPEXevolutionary crystal structure prediction.” Computer Physics Communications 175.11 (2006): 713-720.

[16] Lonie, David C., and Eva Zurek. ”XtalOpt: An open-source evolutionary algorithm for crystal structure prediction.” Computer Physics Communications 182.2 (2011): 372-387.

[17] Tipton, Will, and Richard Hennig. ”GASP: The Genetic Algorithm for Structure and Phase Prediction.”

[18] Revard, Benjamin C., William W. Tipton, and Richard G. Hennig. ”Structure and Stability Prediction of Compounds with Evolutionary Algorithms.” (2014): 1-42.

[19] Mihalkovi, M., et al. ”Total-energy-based prediction of a quasicrystal structure.” Physical Review B 65.10 (2002): 104205.

[20] H.W. Sheng, M.J. Kramer, A. Cadien, T. Fujita and M.W. Chen, Highly-optimized EAM potentials for 14 fcc metals, PRB 83, 134118 (2011)

[21] F. Apostol and Y. Mishin, ”Interatomic potential for the Al-Cu system,” Phys. Rev. B 83, 054116 (2011). DOI: 10.1103/PhysRevB.83.054116

[22] M. Widom and J.A. Moriarty, ”First Principles Interatomic Potentials for Transition Metal Aluminides. II. Application to Al-Co and Al-Ni Phase Diagrams”, Phys. Rev. B 58 (1998) 8967-8979.

[23] Wang, Cai-Zhuang. ”Adaptive Genetic Algorithm for Crystal Structure Prediction.” Conference Manual. 2014.

[24] Ritsch, S., et al. ”The existence regions of structural modifications in decagonal Al-Co-Ni.” Philosophical magazine letters 78.2 (1998): 67-75.

[25] Kob, Walter, and Hans C. Andersen. ”Testing mode-coupling theory for a supercooled binary Lennard-Jones mixture.” Transport Theory and Statistical Physics 24.6-8 (1995): 1179-1198.

[26] Kob, Walter, and Hans C. Andersen. ”Testing mode-coupling theory for a supercooled binary Lennard-Jones mixture. II. Intermediate scattering function and dynamic susceptibility.” Physical Review E 52.4 (1995): 4134.

[27] Amsler, Maximilian, and Stefan Goedecker. ”Crystal structure prediction using the minima hopping method.” The Journal of chemical physics 133.22 (2010): 224104.

[28] Middleton, Thomas F., et al. ”Crystals of binary Lennard-Jones solids.” Physical Review B 64.18 (2001): 184201.

[29] Jones, John Edward. ”On the determination of molecular fields. II. From the equation of state of a gas.” Proceedings of the Royal Society of London A: Mathematical, Physical and Engineering Sciences. Vol. 106. No. 738. The Royal Society, 1924.

[30] Weber, Thomas A., and Frank H. Stillinger. ”Local order and structural transitions in amorphous metal-metalloid alloys.” Physical Review B 31.4 (1985): 1954.

[31] Sheng, H. W., et al. ”Atomic packing and short-to-medium-range order in metallic glasses.” Nature 439.7075 (2006): 419-425.

[32] Li, Zhenqin, and Harold A. Scheraga. ”Monte Carlo-minimization approach to the multiple-minima problem in protein folding.” Proceedings of the National Academy of Sciences 84.19 (1987): 6611-6615.

[33] Wales, David J., and Jonathan PK Doye. ”Global optimization by basin-hopping and the lowest energy structures of Lennard-Jones clusters containing up to 110 atoms.” The Journal of Physical Chemistry A 101.28 (1997): 5111-5116.

[34] D.J.Wales,Cambridge cluster database, http://www-wales.ch.cam.ac.uk/CCD.html

[35] Shechtman, Dan, et al. ”Metallic phase with long-range orientational order and no translational symmetry.” Physical Review Letters 53.20 (1984): 1951.

[36] Frster, Stefan, et al. ”Quasicrystalline structure formation in a classical crystalline thin-film system.” Nature 502.7470 (2013): 215-218.

[37] Stampfli, P. A dodecagonal quasi-periodic lattice in two dimensions. Helv. Phys.Acta 59, 12601263 (1986).

[38] Frster, Stefan, and Wolf Widdra. "Growth, structure, and thermal stability of epitaxial BaTiO 3 films on Pt (111)." Surface Science 604.23 (2010): 2163-2169.

[39] Frster, Stefan, et al. "Epitaxial BaTiO3 (100) films on Pt (100): A low-energy electron diffraction, scanning tunneling microscopy, and x-ray photoelectron spectroscopy study." The Journal of chemical physics 135.10 (2011): 104701.

[40] Frster, Stefan, et al. "Oxygendeficient ordered phases of ultrathin BaTiO3 films on Pt (111)." Surface and Interface Analysis 44.6 (2012): 628-634.

[41] Henrich, Victor E., G. Dresselhaus, and H. J. Zeiger. "Surface defects and the electronic structure of SrTi O 3 surfaces." Physical Review B 17.12 (1978): 4908.

[42] Freeman, Colin L., et al. "A new potential model for barium titanate and its implications for rare-earth doping." Journal of Materials Chemistry 21.13 (2011): 4861-4868.

[43] Tinte, S., et al. "Atomistic modelling of BaTiO3 based on first-principles calculations." Journal of Physics: Condensed Matter 11.48 (1999): 9679.

[44] Wunderlich, Wilfried, Masayuki Fujimoto, and Hitoshi Ohsato. "Molecular dynamics calculations about misfit dislocations at the BaTiO 3/SrTiO 3-interface." Thin Solid Films 375.1 (2000): 9-14.

[45] Elser, Veit, and Christopher L. Henley. "Crystal and quasicrystal structures in Al-Mn-Si alloys." Physical review letters 55.26 (1985): 2883.

[46] Goldberg, David E., and John H. Holland. "Genetic algorithms and machine learning." Machine learning 3.2 (1988): 95-99.

[47] Fischer, Christopher C., et al. "Predicting crystal structure by merging data mining with quantum mechanics." Nature materials 5.8 (2006): 641-646.

99